Supporting Information

Haile et al. 10.1073/pnas.0912510106

SI Text

Quaternary Stratigraphy. The Stevens Village exposure (65° 59'N, 148° 57'W) was examined and described from a cut bank produced by the southward migration of the Yukon River. Excavations were made to frozen sediments (typically 1–2 m laterally into the exposure in July 2005).

The site is 14.5 m high from river level to the modern surface, composed of fluvial sands overlain by loess with seven laterally continuous (>10 m) interbedded organic horizons, identified as paleosols. These paleosols are largely Inceptisols with A/AC/Ck or A/E/Bw/Ck horizons with at least one paleosol trending toward a Spodosol (A/E/Bs/Ck) near the surface of the exposure. The majority of the paleosols show evidence of cryoturbation (i.e., frost cracks and ice wedge casts), while interbedded silts commonly show evidence of syngenetic frost cracks, indicating that permafrost aggraded with the sediments. Permafrost at the site is dry with pore ice estimated at ca. 20–30%; visible ice is absent.

Loess at the site is dominantly medium to coarse silt (≈50–80%) with minor sand. The loess is strongly calcareous, consistent with a Yukon River source (1). As an overall depositional model these silts would originally have been transported as either glacially derived suspended sediment (estimated at >90% of the modern sediment load) (1) or a minor source may be eroded from riverbanks and bars and subsequently deposited on channel bars and floodplains. Following drying, these sediments were deflated by winds and deposited as loess on the river margin. The lateral continuity and repetition of multiple paleosols over the 3 km lateral exposure suggests rapid aggradation associated with an abundant sediment source, or in this case winds blowing off the Yukon River.

The stratigraphy and radiocarbon chronology indicate that loess deposition was episodic through the early Holocene. The exceptional preservation of plant material in growth position associated with several of the soil surfaces suggests that loess aggradation was rapid, and paleosols were buried quickly. In this way we conservatively associate radiocarbon ages from the underlying paleosols with the immediately overlying loess. Given this model, sample DNA30, associated with mammoth, moose, bison, and horse at 12 m, overlies a radiocarbon age of 9,210 ± 25 ^{14}C yr BP (10,260–10,490 yr BP) and is overlain by three ages ranging from ca. 6,950–7,100 ^{14}C yr BP (7,700–8,160 yr BP); we think that the underlying age is a conservative estimate of the true age of DNA30. Unfortunately, we recovered no dateable plant macrofossils from the level of DNA30.

Dating of Exposure. Plant materials were collected either from plants in growth position, or from bulk samples of O and A horizons that were processed for plant macrofossils by wet sieving (Table S1). Radiocarbon ages of associated plant macrofossils were analyzed at the Geological Survey of Canada (radiometric ages, GSC prefix), University of Arizona (AMS ages, AA prefix), or the Keck AMS facility at the University of California-Irvine (AMS ages, UCIAMS prefix).

OSL dating provides an estimate of the time since luminescent minerals, such as quartz, were last exposed to sunlight (2, 3). Sediment samples were collected from cleaned sections using opaque PVC tubes, and the outer few centimeters of material at the tube ends were discarded in the laboratory to remove any light-exposed grains. Quartz grains of 90–125 μm in diameter were extracted from the remaining material under safelight conditions and prepared for dating using standard procedures (2). Individual grains were stimulated by green laser light, and the equivalent dose (D_e) was estimated from the UV emissions using the same instrumentation, single-aliquot regenerative-dose protocol, and associated grain-rejection criteria as described elsewhere (4, 5). The natural, regenerative, and test doses were preheated at 180 °C for 10 s before optical stimulation; these conditions yielded a ratio consistent with unity (0.999 ± 0.023) for five multigrain aliquots of sample SV30 subjected to a dose-recovery test. The latter involved an initial optical bleach of the natural OSL signal using blue light-emitting diodes (two successive illuminations, each of 1,000 s duration, at ambient temperature), before applying a known β dose to act as the surrogate natural dose. OSL decay and dose-response curves for two grains are shown in Fig. S1. The D_e values of two and seven grains of samples SV28 and SV26, respectively, were estimated by extrapolating the dose-response curve beyond the largest given regenerative dose, but the OSL ages of these samples are not sensitive to the inclusion or rejection of these grains.

The burial dose of each sample was determined from the individual D_e estimates using the four-parameter minimum age model (6). The choice of model was based on goodness-of-fit criteria and was used because of the wide spread in D_e values for all three samples (Fig. S2). The associated overdispersion values of 70–80% (Table S2) are much higher than those commonly reported for well-bleached sediments that have remained undisturbed since burial (<20%). We attribute the overdispersion to insufficient bleaching at the time of deposition (7), because these well-laminated and perennially frozen sandy silts are unlikely to have suffered from postdepositional mixing. This interpretation implies that these aeolian grains were derived from local sources and transported over short distances (8).

OSL ages (Table S2) were calculated by dividing the burial doses by the dose rates due to ionizing radiation from ^{238}U, ^{235}U, ^{232}Th (and their decay products), and ^{40}K, with a small contribution from cosmic rays. Concentrations of U, Th, and K in dried and powdered samples were measured using a combination of instrumental neutron activation analysis (INAA) and inductively coupled plasma optical emission spectroscopy (ICP-OES), supplemented by β-counting to establish that significant disequilibrium is not present in the U or Th decay chains. Because the sediments have remained frozen since deposition, we assumed that the measured concentrations and field water contents have prevailed throughout the period of sample burial. Other aspects of dose rate determination follow previous studies (4, 5), but also allow for dose-rate attenuation by organic matter (9).

DNA Methodology. In Copenhagen, DNA extractions followed established protocols (10). In Oxford, a protocol was applied that allows for DNA extraction of larger sediment quantities. Approximately10 g wet weight of frozen sediment was subsampled, placed in PowerMax Soil PowerBead tubes (Cambio), and dissolved in 24 mL lysis buffer (11). The tubes were then agitated vigorously for 1 min and left to incubate overnight at 65 °C under gentle agitation. Following extraction, the DNA was purified using the PowerMax Soil DNA Isolation kit protocol, before being concentrated with Amicon Ultra 30 kDa spin columns.

Initially shotgun sequencing by Roche GS 20 DNA sequencing platform was attempted on two Pleistocene permafrost samples from Ice Bluff, Main River, Siberian Beringia that are much richer in megafauna *sed*aDNA than the Stevens Village site. As all identifiable sequences were found to be of microbial origin, likely due to an enormous microbial DNA load compared to that

of higher organisms, we abandoned this approach. Instead, PCR was used to amplify various mammal mtDNA sequences using both species-specific and generalized mammal primers (Table S3). It is noteworthy that mtDNA control region sequences were attempted to be amplified from horse (as was done for mammoth), but unsuccessfully. In another project on Pleistocene horses (macrofossils) from the Americas, we have noticed a substantial variation in the control region sequences. This makes it very hard to design primers for the amplification of short sequences within this region, and may well be the reason for our failure.

Two microliters DNA extract were subjected to 55–60 cycles of PCR (1.5 min initial denaturation at 97 °C, 45 s at 94 °C, 45 s at 56–60 °C, 1.5 min at 68 °C, and a final cycle of 10 min at 68 °C). Given the concern of contaminant human DNA "masking" endogenous animal DNA, we incorporated a 10-fold excess of human-specific blocking probes (12) into the 16S analysis. PCR products were cleaned using a QIAquick PCR Purification kit (Qiagen). The initially examined amplification products were cloned and sequenced using the conventional Sanger approach on ABI chemistry by the commercial Macrogen facility (Macrogen). To obtain larger numbers of cloned products, 21 of the PCR products were additionally sequenced on the Roche FLX DNA sequencing platform (Copenhagen). FLX library build and sequencing was principally following the manufacturer's guidance, although with the following modifications: The nebulization and AMPure purification steps were omitted, and the last NaOH melting step was replaced by a heat-treatment (13). During the library build, MID tags were incorporated to the PCR products grouped equimolarly by layer. Each group of PCR products was ligated to a different MID tag, which subsequently enabled the pooling of the products at equimolar ratio into a final single DNA pool. A large region of a LR70 FLX sequencing run was performed on this pool, generating 226,307 reads after standard instrument filtering. Subsequently, sequences were sorted based on MID tags and primer sequences, allowing, respectively, one or two mismatches, thus bringing the total of sequences to 134,084.

Control Samples. In August 2009, we collected 17 samples of Yukon River water, 12 surface sediment samples on river bars near exposures of late Pleistocene and Holocene sediment, and 10 samples of modern soil at the Stevens Village *sed*aDNA site. Sampling sites in the lower Yukon Flats are shown in Fig. S4, and sample details are provided in Table S5. All samples were collected in duplicate.

Samples were collected in sterile 50-mL plastic centrifuge tubes that were then bagged in sterile Whirlpaks. Water samples were collected by immersing centrifuge tubes in river water from a boat near the center of the channel. River bar surface sediments were collected by scraping the centrifuge tube through the uppermost 1 cm (approximately) of surface silt and sand. At each river bar, we collected four samples along a slope transect starting just above river level and ending in riparian shrub thickets (typically shrubby *Salix* spp.). Soil samples were collected at five sites from the modern soil at the top of the Stevens Village exposure, near the *sed*aDNA sampling site. Soil O and A horizons were sampled with a trowel that was cleaned before each use by immersion in bleach followed by rinsing with distilled water. DNA was extracted and amplified in the same manner as the *sed*aDNA samples from the Stevens Village exposure.

Taxonomic Assignments. Sequences were assigned to taxon using the program SAP (vers. 1.0.2) (14, 15). In short, for each unique query permafrost DNA sequence a set of up to 50 homologs sequences were compiled using BLAST searches via GenBank and annotations from the National Center for Biotechnology Information (NCBI) taxonomy browser. This is carried out in such a way that both the closest homologs as well as homologs representing a wider range of relevant taxa are included. Analysis was only continued if the set included at least one BLAST hit with an E value below 0.1. The homologs sequences were aligned using ClustalW2, and a version of the Neighbor-joining algorithm allowing topological constraints on trees (15) was applied to the alignment. One thousand trees were sampled using bootstrapping.

The probability that a query sequence belongs to a given taxon was approximated as the proportion of bootstrap trees, where the query sequence and the homologs representing the taxon in question form a monophyletic group.

In cases where a species is not sequenced for the marker in question a valid species level assignment cannot be made. For this reason, SAP aborts the analysis unless at least one homolog meets a minimum sequence identity criterion. The default value of this parameter is 95% and serves to describe an upper bound to the within-species diversity expected.

Sequences proving identifiable by SAP were additionally identified by BLAST search against GenBank, notifying the taxon with the highest hit (Table 1) as well as the sequences of other closely related taxa (Fig. S3).

Additionally, to the taxa presented in Table 1, sequences assigned to taxa of typical laboratory contaminates (16) were occasionally recovered and omitted. These included human (*Homo*), pig (*Sus*), rabbit (*Oryctolagus*), cow (*Bos*), and mouse (*Mus*).

Statistical Modeling of Macrofossil Ages. We tabulated the 164 reliably dated mammoth macrofossils from Alaska/Yukon with ages of <35,000 calendar years before present (yr BP) (Table S4). Fossils older than this were excluded, as they are often difficult to date reliably. We then calculated the probability of not yet having recovered any fossils ranging in age from 13,100–10,260 yr BP: the youngest age of the mammoth macrofossils and permafrost mammoth *sed*aDNA, respectively (Table S4 and Fig. 2). A model of constant rate of macrofossil deposition was assumed; as was a population density decrease by a factor $1/\alpha$ after 13,100 yr BP and a hypothetical termination at 10,260 yr BP. Under these assumptions, the probability of not yet having recovered mammoth macrofossils between 13,100 and 10,260 yr BP is:

$$\Pr(n_\alpha = 0) = \left(\frac{35{,}000 - 13{,}100}{35{,}000 + (\alpha - 1)13{,}100 - \alpha 10{,}260)}\right)^{164}$$

The probability of observing no macrofossils from 13,100–10,260 yr BP is shown for various values of $1/\alpha$ in Fig. 2.

We also applied a standard parametric method used for estimating the SLE, which incorporates fossil recovery rates, to: (*i*) estimate the lower statistical confidence bound of extinction using the macrofossil data ($n = 164$) and (*ii*) to infer the reduction in recovery rate required for a >50% probability of failing to recover a macrofossil in the interval 13,100–10,260 yr BP.

The extinction model used was:

$$p = (1 - r)^i,\ r = n/t_n,$$

Where n is the number of samples, t_n is the time interval of fossil recovery, i is the time interval between the last recovered fossil and the inferred extinction date, and p is the probability of persistence over i (17). This equation yields a lower 95% confidence bound of 12,696 yr BP, under the assumption that the population size of Alaskan mammoth (and hence macrofossil recovery rate) remained constant through to extinction. However, as noted previously, if population density was reduced before extinction, this estimate would be biased toward an overly

old age. As such, we can estimate the reduction in density (D_r), via a reduction in r (assuming $r \propto D$), required for any given probability of persistence (p):

$$D_r = \frac{r}{1 - \exp(\log(p = 0.5)/i)}$$

This method suggests a 33-fold reduction in macrofossil recovery rate (and hence density) would have been required for the probability of persistence through to 10,260 yr BP to be 50%. For $P \geq 5\%$, a 7.6-fold reduction is required.

Authenticity of Results. The *sed*aDNA approach raises the question of whether the horse and mammoth DNA recovered from the sediments is primary and, hence, of Holocene age. A number of observations validate this interpretation, as discussed below.

River-Deposited *sed*aDNA. The sediments at the Stevens Village site consist of sandy loess (wind-blown silt) derived from the floodplain of the Yukon River. These floodplain silts would have accumulated either as sediment derived from glacial melt water in the headwaters of the Yukon River, the single largest source of modern sediment transported by the Yukon River (>90% of the modern sediment load) (18–20), or from the erosion of river cut banks and redeposition of sediment on river bars. In either case, these fine-grained sediments were transported by water, deposited on bars where they were dried, and subsequently deflated and transported on to the surface of the Stevens Village site (a 3-km-wide exposure of laterally continuous paleosols with interbedded silts). Previous experiments at a similar site (albeit much richer in *sed*aDNA: Ice Bluff, Main River, Siberian Beringia) show that while *sed*aDNA of megafauna can be obtained from primary loess sediments, it could not be amplified successfully from either the river water or from water-borne sediments, even when collected adjacent to the exposure (21). This observation was confirmed by testing for DNA in 17 samples of river water and 12 samples of river bar surface sediments taken upstream, downstream, and directly below the Stevens Village site. None of these samples yielded putative megafauna DNA. It seems unlikely, therefore, that our *sed*aDNA findings at Stevens Village are the result of river redeposition.

Wind-Deposited *sed*aDNA. DNA extracted from samples of modern, undisturbed surface sediment, collected from several localities in Arctic and temperate regions, has yielded the genetic signatures of extant fauna only (10, 21–23). This suggests that *sed*aDNA is not readily reworked from older deposits and incorporated into younger deposits. In addition, a series of ice-core samples from Greenland showed no evidence of wind-borne transport of *sed*aDNA. That is, plant and animal *sed*aDNA studies of basal silty ice (icy permafrost) from deep ice cores indicated the past existence of diverse plant and animal communities, but similar results could not be obtained from ice samples taken from above these basal layers. The upper layers are derived from compressed wind-blown snow and contain various inorganic particles. The fact that no associated *sed*aDNA of plants or animals was recovered from the upper layers suggests that long-distance, wind-borne transport of DNA coupled to inorganic particles is not a likely source of *sed*aDNA (23). Further evidence against wind-borne transport of DNA is provided by sediment samples collected from temperate regions. For example, although moa *sed*aDNA derived from multiple species has been recovered from sediments located in different rock shelters in New Zealand, a clear pattern can be observed that links the appropriately sized species with the appropriately sized shelter. This outcome would not be expected if the *sed*aDNA had been dispersed by the wind (22). We directly tested for the possibility of wind-blown *sed*aDNA contaminants in the Stevens Village samples by attempting amplifications on 10 surface soil samples collected from around the study site. None of these samples produced any megafauna DNA sequences. This result provides reassurance that the traces of mammoth and horse *sed*aDNA preserved at Stevens Village are contemporaneous with the Holocene sediments from which they were recovered and are not an artifact of reworking of Pleistocene *sed*aDNA by modern aeolian processes.

Local Sources of Contaminant *sed*aDNA. The sediments surrounding the Stevens Village site are largely Holocene in age (18). The stratigraphy of the Yukon Flats basin, which includes the Stevens Village site, consists of a largely Holocene scrolled Yukon River floodplain incised into a terminal Pleistocene aeolian sand sheet complex (18, 19). Radiocarbon ages on the sand sheets suggest most were active ≈10,300–10,200 radiocarbon yr BP (^{14}C yr BP), with only one sand sheet dated slightly earlier (11,500 ^{14}C yr BP) ≈30 km upstream from Stevens Village (1). One could argue that other late Pleistocene sites may exist along the river and were not sampled in previous studies, but we would maintain that they are not common. Thus, any possible sediment sources of Pleistocene contamination must, at the worst, be considered extremely rare.

DNA Leaching and Mobility. Mammoth and horse *sed*aDNA were found only in a single stratum at Stevens Village (Fig. 1). This finding suggests that *sed*aDNA is not vertically transported readily between layers under permafrost conditions. The youngest macrofossil ages for mammoth and horse in Alaska/Yukon are several millennia older than the stratum from which we recovered the *sed*aDNA of these two species at Stevens Village, corresponding to deposits more than 8 m deeper in the stratigraphic sequence (see Fig. 1). It is highly improbable that mammoth and horse *sed*aDNA could have moved upwards over this distance, through frozen strata, and without leaving any traces of either species behind in the intervening sediments.

Although some downward leaching of DNA has been observed in nonfrozen settings (22), our finding is consistent with a number of studies showing no evidence of DNA movement between strata where permafrost is present or was present recently (23–27) Specifically, clear reverse correlations have been found between *sed*aDNA damage (24, 25), microbial diversity (24, 26) and age of permafrost cores, while no such correlations have been found with core depth, opposite to the findings reported for some nonfrozen sites where DNA leaching was detected (22). Likewise, where comparable, the *sed*aDNA faunal record (estimated quantitatively by real-time PCR) follows that of the corresponding fossil bone record and shows no relationship to sample depth (27). Finally, ice sampled just above that of icy permafrost (silty ice) rich in animal and plant *sed*aDNA returned negative results for such taxa, despite minor amounts of free water being present (23).

It is unlikely that DNA associated with Pleistocene-age groundwater has contaminated the sediments at Stevens Village. Stable oxygen isotope ratios of permafrost pore ice from the Stevens exposure are consistent with Holocene meteoric water sources. The mean and standard deviation of pore ice δ^{18}O values in the sediments sampled for *sed*aDNA is $-22.1 \pm 0.7‰$ (VSMOW) comparable to modern values in the region. For comparison, early-Holocene ground ice and sediment pore ice in the Klondike region of adjacent Yukon have δ^{18}O values ranging between approximately -24 to $-20‰$. In contrast, samples dating to the late Pleistocene are isotopically lighter, with values between approximately -32 to $-29‰$ (28).

We could expect there may have been some mixing in the paleoactive layer at the Stevens Village site, but based on translocation of A-horizon material and frost cracks, we would estimate this at ≈30- to 50-cm depth.

Observed Distribution Pattern Makes Secondary Transport Unlikely. Within the sediments, *sed*aDNA from horse and multiple individuals of mammoth were recovered from the same layer (mammoth DNA from multiple cores from the same layer) and that of both species from only one of 15 layers investigated (spanning 4,000 years of deposition). The chance of such "concentrated" findings resulting from secondary-transported *sed*aDNA is considered unlikely, given that the deposits have a similar depositional history; further, multiple *sed*aDNA amplification products from each layer underwent in-depth FLX sequencing that should reveal *sed*aDNA from all mammalian taxa present. The additional finding of moose *sed*aDNA in the same layer as mammoth and horse further supports a Holocene age for the *sed*aDNA sequences. Moose is mainly considered a Holocene mammal in Yukon and Alaska. We consider it improbable that identification of multiple individuals of mammoth, horse, and moose in the same layer indicates the redeposition of mammoth and horse DNA, while that of moose is in primary context, given the low frequency at which the *sed*aDNA of all three species occur at the site. Further, mammoth *sed*aDNA was obtained in multiple amplifications using universal mammalian 16S mtDNA primers (known to amplify DNA from a variety of mammals) (e.g., 10) (Table S3), whereas moose and hare *sed*aDNA were amplified less frequently from the same layer using the same primers. This suggests that mammoth *sed*aDNA is at least as abundant as that of moose and hare, even though these extant species are known to have been present throughout the entire period of sedimentation; thereby supporting the contention that mammoth *sed*aDNA is not simply a minor contaminant in a layer with putative moose and hare DNA.

Mammoth Results Reproduced Independently. DNA assigned to mammoth could be reproducibly recovered in Copenhagen (Gilbert) and Oxford (Haile) from the Stevens Village permafrost using 16S and control region mtDNA markers. Reproducibility of the mammoth results by independent laboratories indicates that the finding is not due to laboratory contamination (29), especially given that the North American mammoth C haplogroup has not previously been worked on in the two laboratories.

Interestingly, studies have shown that the vast majority of DNA in sediments is in an extracellular stage, either as naked molecules or bound to inorganic particles (30). DNA being a relatively unstable molecule compared to most other cellular components (31, 32), it is likely that any *sed*aDNA exposed to the surrounding environment may undergo rapid degradation through oxidation, hydrolysis, and/or UV irradiation, which may be the reason for the lack of evidence of *sed*aDNA being commonly redistributed in the environment.

Other Contexts for *sed*aDNA Analyses. To exploit fully the utility of *sed*aDNA analysis in paleontological and paleoenvironmental studies, and to understand its technical and geographical limitations, it will be necessary to conduct further analyses, in a variety of depositional contexts and landscapes. Although it is clear that localities situated in cold climates will always be preferred for ancient DNA recovery, conditions suitable for preservation might also be found in dry temperate regions (such as steppe or plains), certain kinds of cave environments, and even the tropics (Fig. 3). But for all sites, reliable dating procedures and a clear understanding of the geomorphic context and depositional history will be critical. For a companion study similar to this one, conducted on sediments collected from a small thermokarst lake on the western side of Lake Taimyr in arctic Siberia, we used both OSL and radiocarbon dating. However, macrofossils, such as recognizable plant pieces, were in short supply at this locality, and age estimates for equivalent horizons using macrofossils, bulk sediments, and OSL were not in good agreement overall. Although molecular signals indicated a rich diversity of late Quaternary taxa, including mammoths, the mismatch in age estimates for comparable surfaces within the lake sediments precluded further analysis. Interpretation of the *sed*aDNA results was complicated further by the fact that thermokarst pond environments are prone to slumping and redistribution of old sediments, potentially resulting in redeposition of *sed*aDNA. At this Siberian site, therefore, we could not establish with confidence that the *sed*aDNA recovered from the sediments was contemporaneous with the dated materials.

1. Muhs DR, Budahn JR (2006) Geochemical evidence for the origin of late Quaternary loess in central Alaska. *Can J Earth Sci* 43:323–337.
2. Aitken MJ (1998) An Introduction to Optical Dating (Oxford University Press, Oxford, UK).
3. Lian OB, Roberts RG (2006) Dating the Quaternary: Progress in luminescence dating of sediments. *Quat Sci Rev* 25:2449.
4. Arnold LJ, et al. (2008) Optical dating of perennially frozen deposits associated with preserved ancient plant and animal DNA in north-central Siberia. *Quat Geochron* 3:114–136.
5. Demuro M, et al. (2008) Optically stimulated luminescence dating of single and multiple grains of quartz from perennially frozen loess in western Yukon Territory, Canada: Comparison with radiocarbon chronologies for the late Pleistocene Dawson tephra. *Quat Geochron* 3:346–364.
6. Galbraith RF, et al. (1999) Optical dating of single and multiple grains of quartz from Jinmium rock shelter, northern Australia: Part I, experimental design and statistical models. *Archaeometry* 41: 339–364.
7. Olley JM, et al. (2004) Optical dating of Holocene sediments from a variety of geomorphic settings using single grains of quartz. *Geomorphology* 60:337–358.
8. Lian OB, Huntley DJ (1999) Optical dating studies of post-glacial aeolian deposits from the south-central interior of British Columbia, Canada. *Quat Sci Rev* 18:1453–1466.
9. Lian OB, et al. (1995) Optical dating studies of Quaternary organic-rich sediments from southwestern British Columbia and northwestern Washington State. *Can J Earth Sci* 32:1194–1207.
10. Willerslev E, et al. (2003) Diverse plant and animal genetic records from Holocene and Pleistocene sediments. *Science* 300:791–795.
11. Bulat S, et al. (2000) Identification of a universally primed-PCR-derived sequence-characterized amplified region marker for an antagonistic strain of *Clonostachys rosea* and development of a strain-specific PCR detection assay. *App Environ Microbiol* 66:4758–4763.
12. Rasmussen M, et al. (2009) Response to Comment by Goldberg, et al. on "DNA from pre-Clovis human coprolites in Oregon, North America" *Science* 325:5937.
13. Maricic T, Pääbo S (2009) Optimization of 454 sequencing library preparation from small amounts of DNA permits sequence determination of both DNA strands. *Biotechniques* 46:51–57.
14. Munch K, et al. (2008) Fast phylogenetic DNA barcoding. *Phil Trans R Soc B Biol Sci* 363:3997–4002.
15. Munch K, et al. (2008) Statistical assignment of DNA sequences using Bayesian phylogenetics. *Syst Biol* 57:750–757.
16. Leonard JA, et al. (2007) Animal DNA in PCR reagents plagues ancient DNA research. *J Arch Sci* 34:1361.
17. McInerny G, et al. (2006) Significance of sighting rate in inferring extinction and threat. *Conser Biol* 20:562–567.
18. Froese DG, et al. (2005) Characterizing large river history with shallow geophysics: Middle Yukon River, Yukon Territory and Alaska. *Geomorphology* 67:391–406.
19. Brabets T, et al. (2000) Environmental and Hydrologic Overview of the Yukon River Basin, Alaska and Canada. Anchorage, Alaska (US Department of the Interior, US Geological Survey, Washington, DC).
20. Williams JR (1962) Geologic Reconnaissance of the Yukon Flats District, Alaska (US Geological Survey, Washington DC).
21. Haile J (2009) Ancient DNA from Sediments and Associated Remains (Oxford University Press, Oxford, UK).
22. Haile J, et al. (2007) Ancient DNA chronology within sediment deposits: Are paleobiological reconstructions possible and is DNA leaching a factor? *Mol Biol Evol* 24:982–989.
23. Willerslev E, et al. (2007) Ancient biomolecules from deep ice cores reveal a forested southern Greenland. *Science* 317:111–114.
24. Willerslev E, et al. (2004) Long-term persistence of bacterial DNA. *Curr Biol* 14:R9–R10.
25. Hansen AJ, et al. (2006) Crosslinks rather than strand breaks determine access to ancient DNA sequences from frozen sediments. *Genetics* 173:1175–1179.
26. Johnson SS, et al. (2007) Ancient bacteria show evidence of DNA repair. *Proc Natl Acad Sci USA* 104:14401–14405.
27. Hebsgaard MB, et al. (2009) The farm beneath the sand—an archaeological case study on ancient 'dirt' DNA. *Antiquity* 83:430–444.
28. Kotler E, Burn CR (2000) Cryostratigraphy of the Klondike "muck" deposits, west-central Yukon Territory. *Can J Earth Sci* 37:849–861.
29. Willerslev E, Cooper A (2005) Ancient DNA. *Proc R Soc B* 272:3–16.
30. Trevors JT (1996) DNA in soil: Adsorption, genetic transformation, molecular evolution and genetic microchip. *Antonie Van Leeuwenhoek Int J Gen Mol Microbiol* 70:1–10.

31. Willerslev E, Hansen A, Poinar H (2004) Isolation of nucleic acids and cultures from fossil ice and permafrost. *Trend Ecol Evol* 19:141–147.
32. Lindahl T (1993) Instability and decay of the primary structure of DNA. *Nature* 362:709–715.
33. Taylor PG (1996) Reproducibility of ancient DNA sequences from extinct Pleistocene fauna. *Mol Biol Evol* 13:283–285.
34. Guthrie RD (2006) New carbon dates link climatic change with human colonization and Pleistocene extinctions. *Nature* 441:207–209.
35. Burney DA, Flannery TF (2005) Fifty millennia of catastrophic extinctions after human contact. *Trend Ecol Evol* 20:395–401.
36. Koch PL, Barnosky AD (2006) Late Quaternary extinctions: State of the debate. *Ann Rev Ecol Evol Syst* 37:215–250.
37. MacPhee R, Marx P (1997) in *Natural Change and Human Impact in Madagascar*, eds Goodman SM, Patterson B (Smithsonian Inst Press, Washington, DC) pp 169–217.

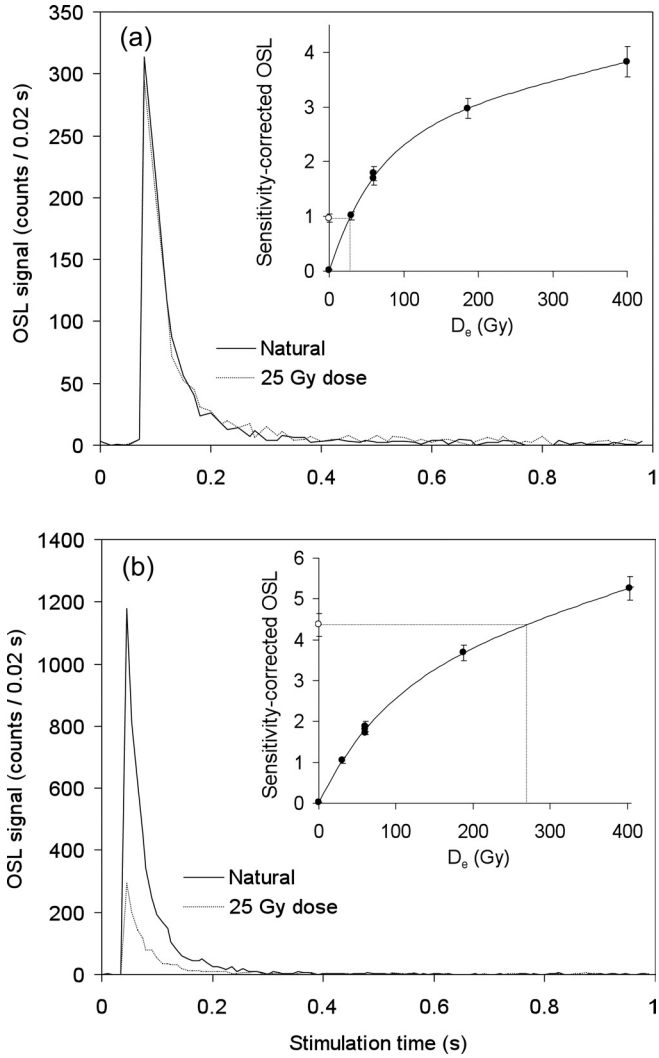

Fig. S1. Example OSL decay curves and dose-response curves (inset plots) for two individual grains of quartz from sample SV28: (*A*) grain with D_e of 27 ± 3 Gy, and (*B*) grain with D_e value of 271 ± 34 Gy. OSL decay curves are shown for the natural doses (solid lines) and for regenerative doses of 25 Gy (dashed lines), following heating to 180 °C for 10 s. The laser was not switched on during the initial or final 0.08 s of stimulation. In the inset plots, the open circles (on the *y* axis) and filled circles denote the natural and regenerated OSL signals, respectively. Dose-response curves (solid lines) were fitted to the regenerative-dose points using a single saturating-exponential-plus-linear function to estimate the D_e values (read off the *x* axis; dashed lines).

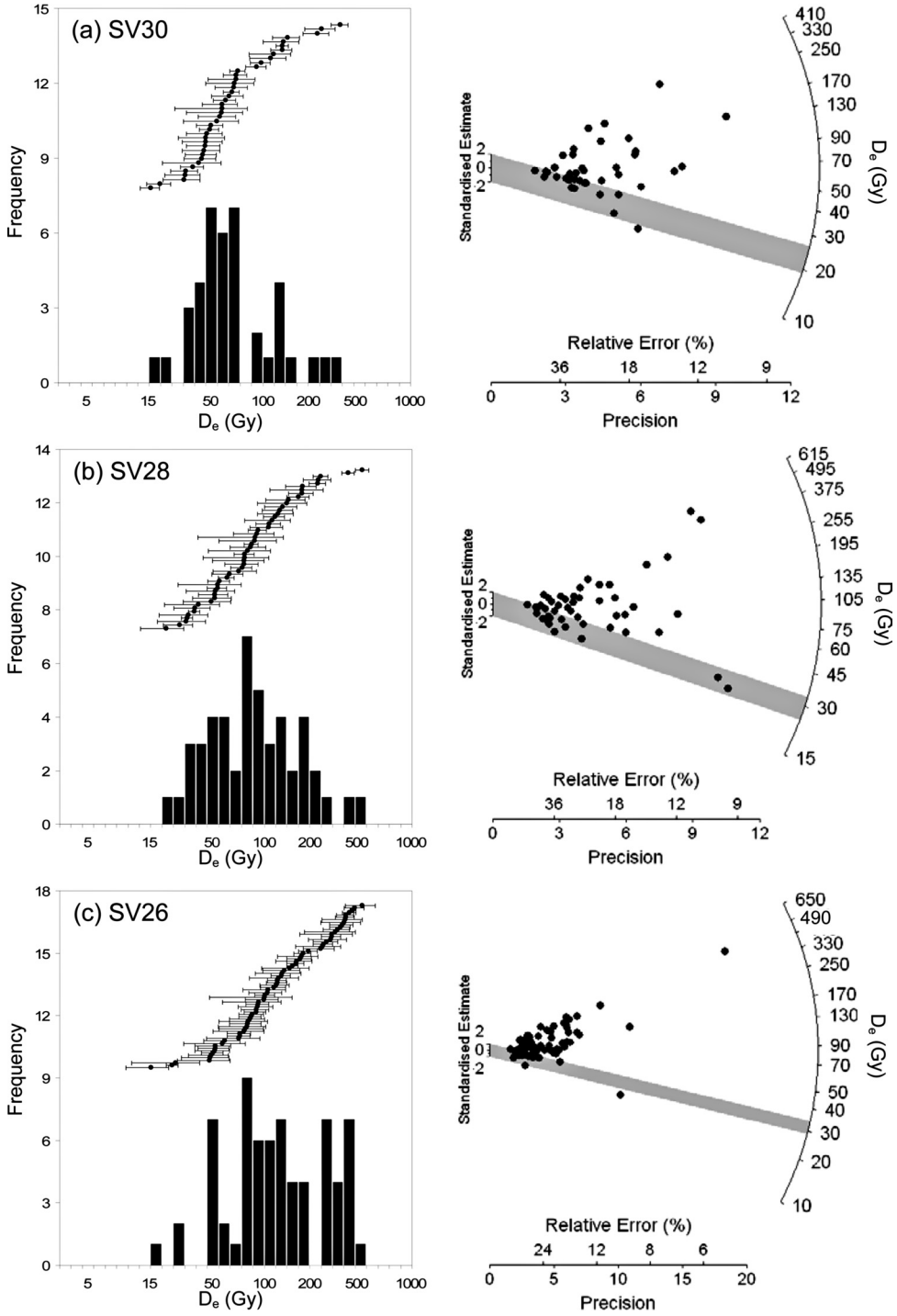

Fig. S2. Single-grain D_e distributions for the three OSL samples, shown as frequency histograms (using a log scale for the *x* axis) and radial plots. If the spread in D_e estimates were due solely to measurement error, then 95% of the data points in the radial plots should be captured by any chosen band of ± 2 units extending from the standardized estimate axis. The gray bands shown here are centered on the D_e values used to calculate the OSL ages.

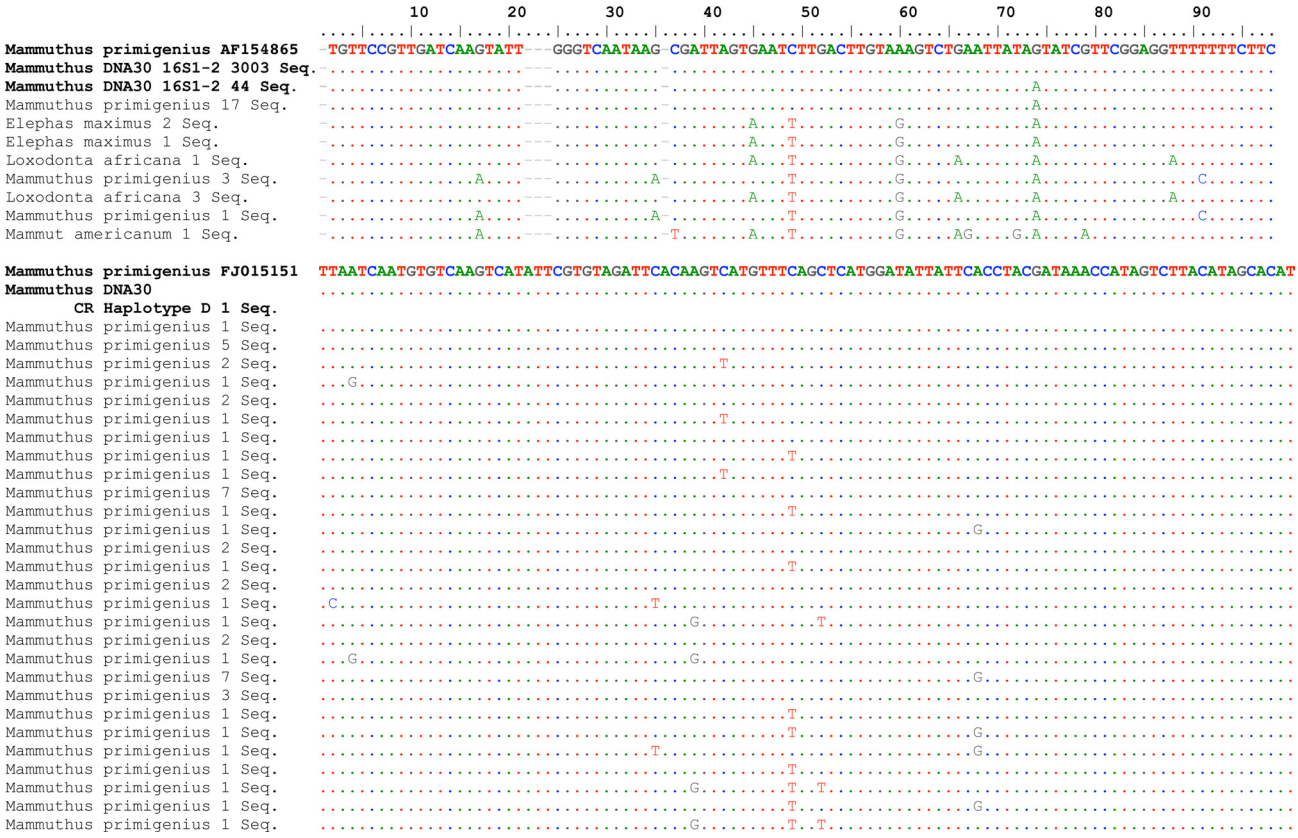

Fig. S3. Alignment of query sequences identified by SAP with sequences in GenBank, showing the highest BLAST hit.

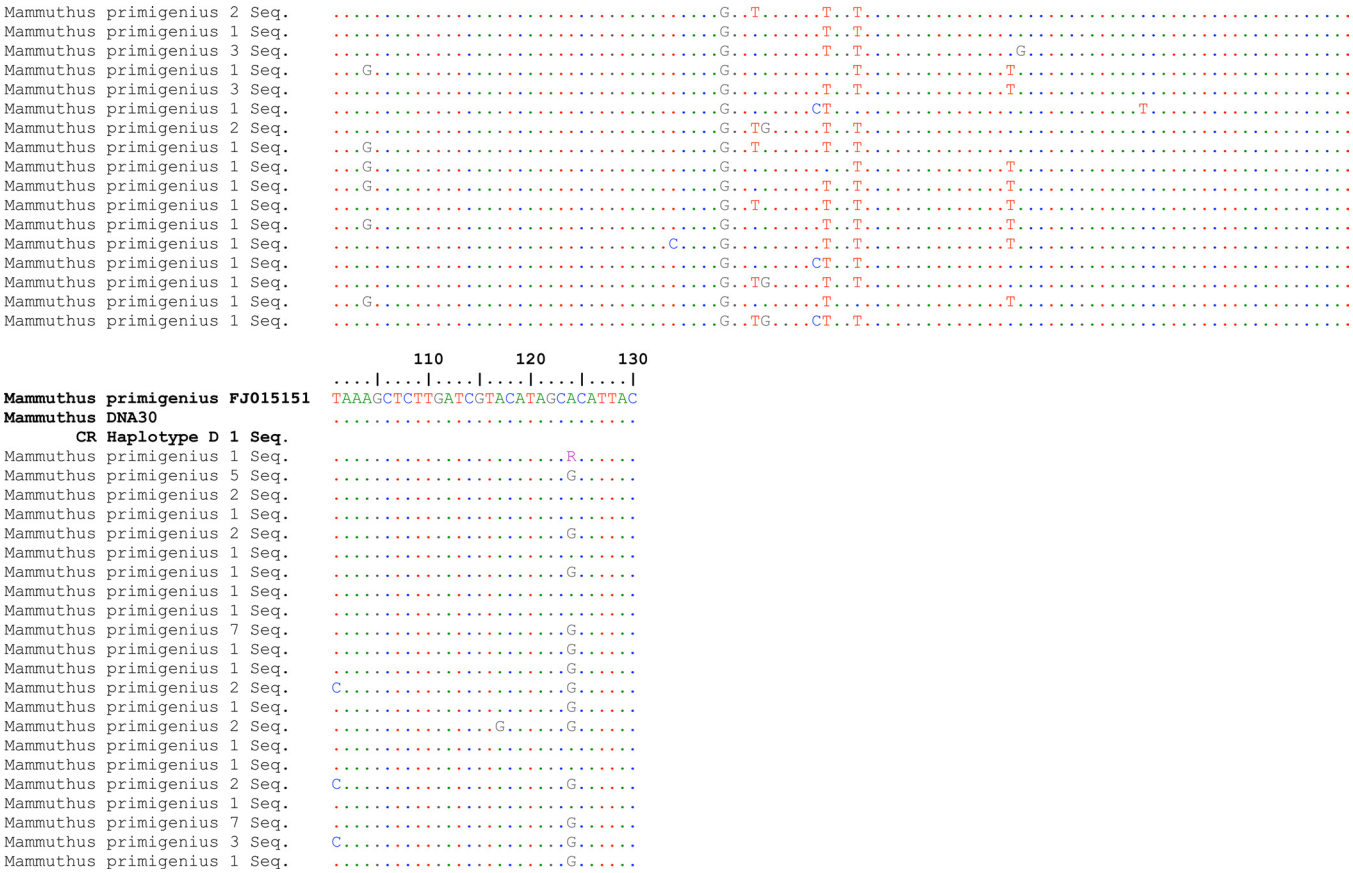

Fig. S3. continued.

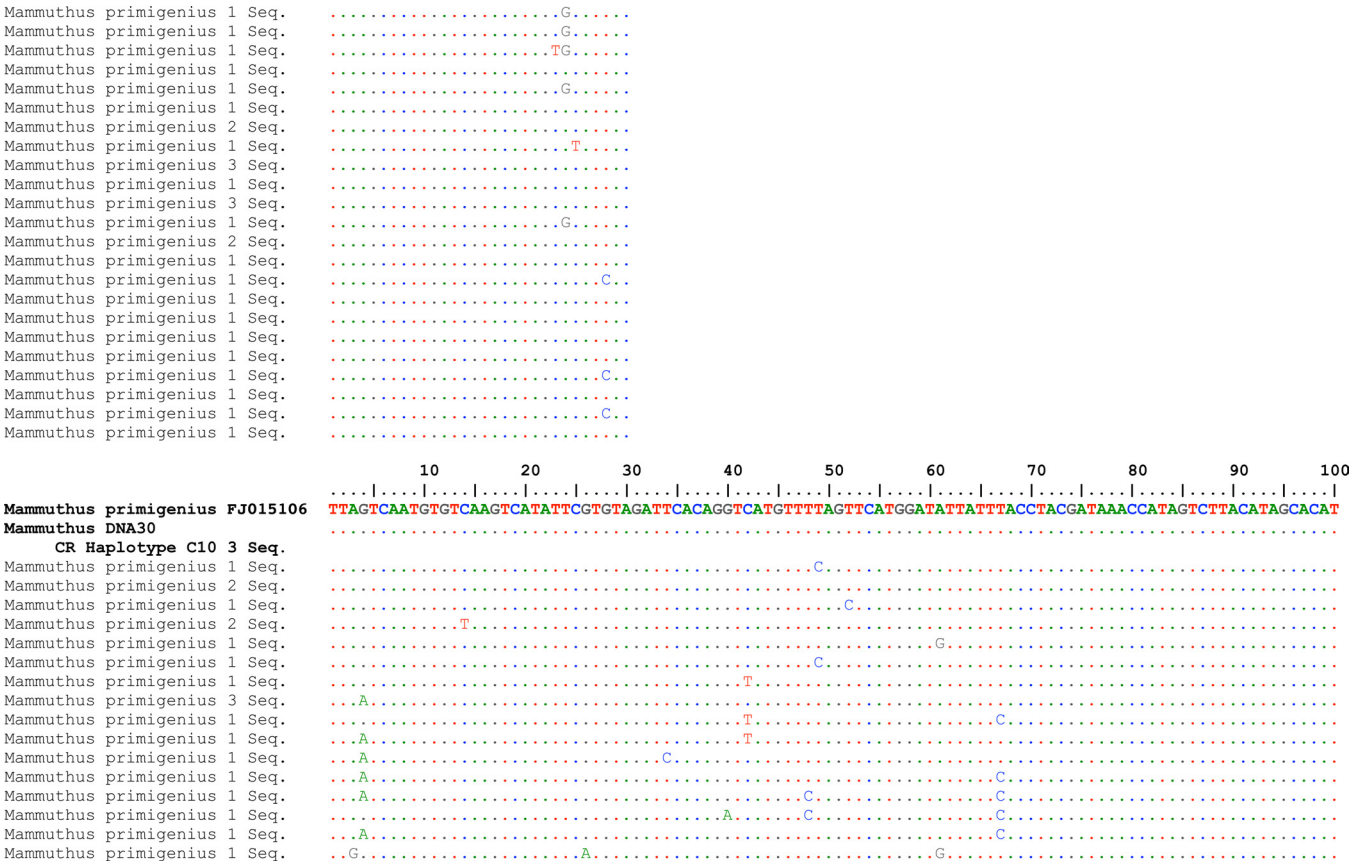

Fig. S3. continued.

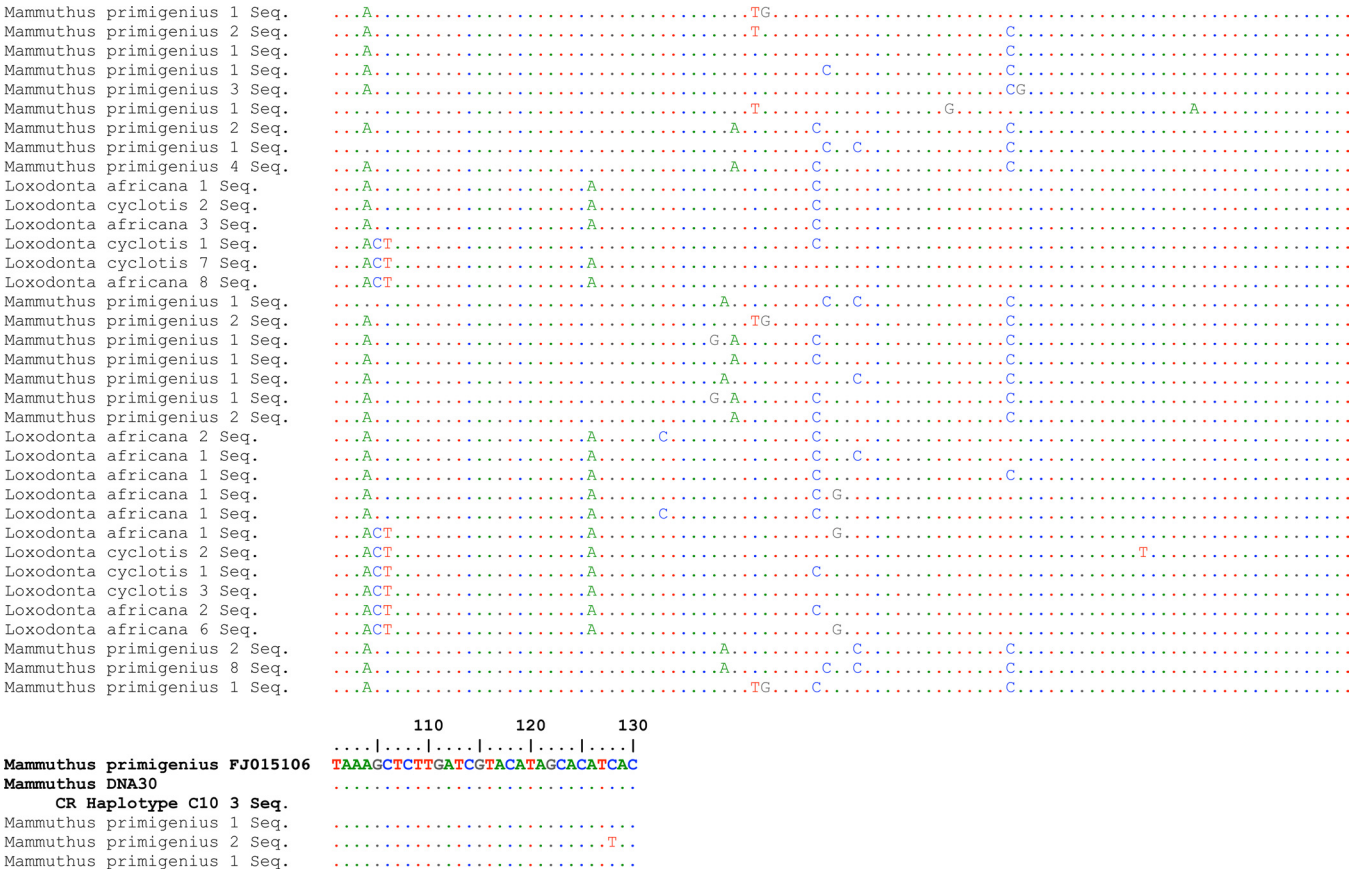

Fig. S3. continued.

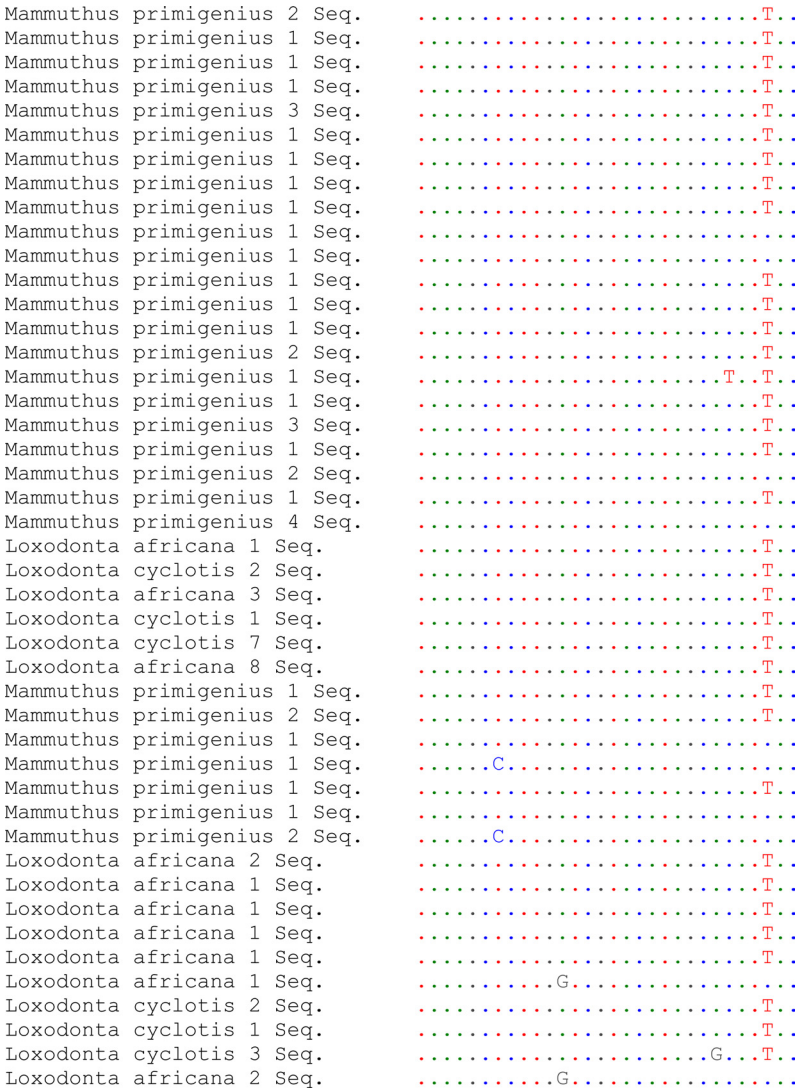

Fig. S3. continued.

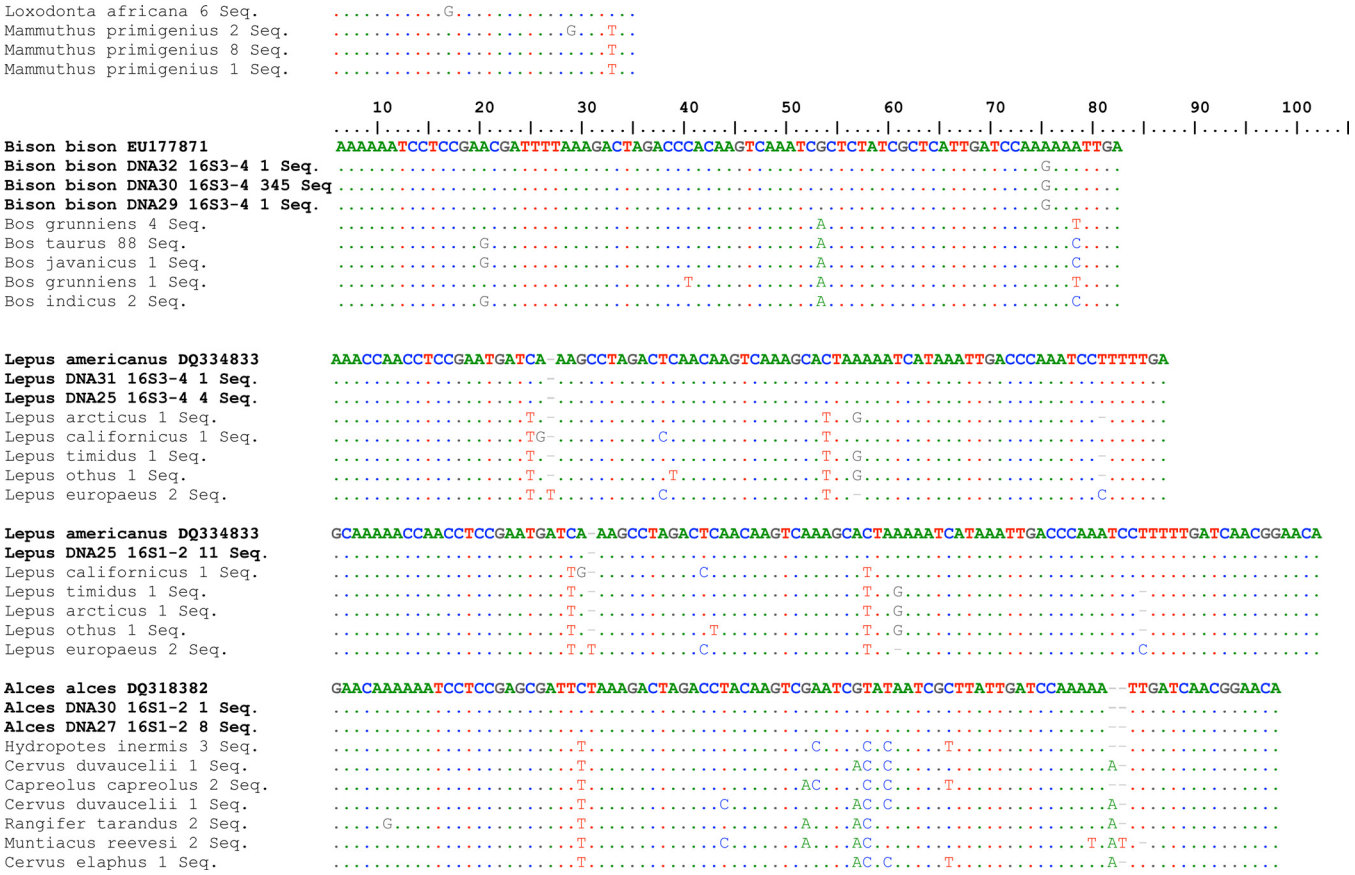

Fig. S3. continued.

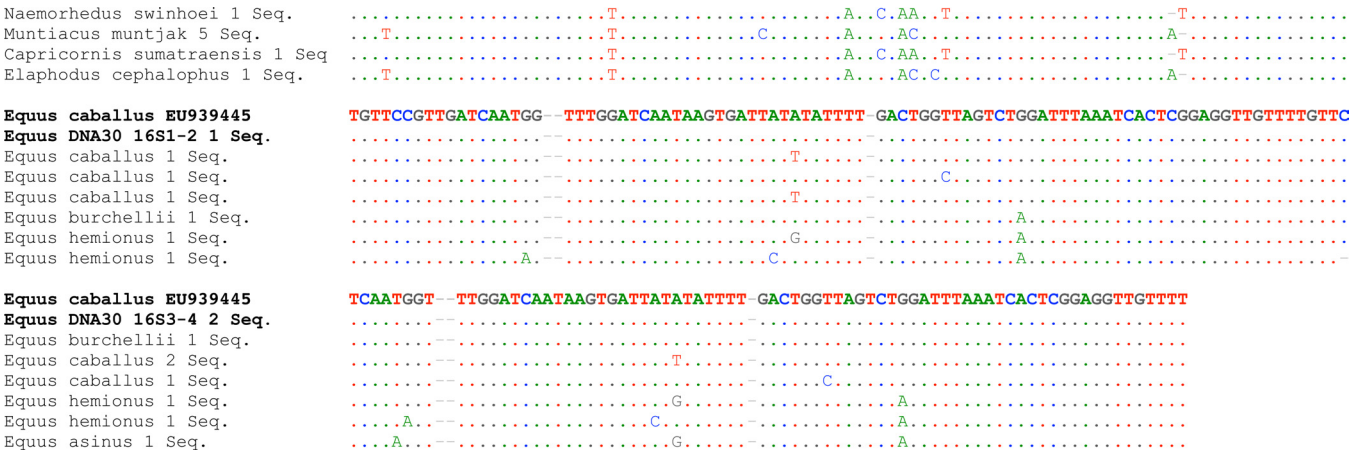

Fig. S3. continued.

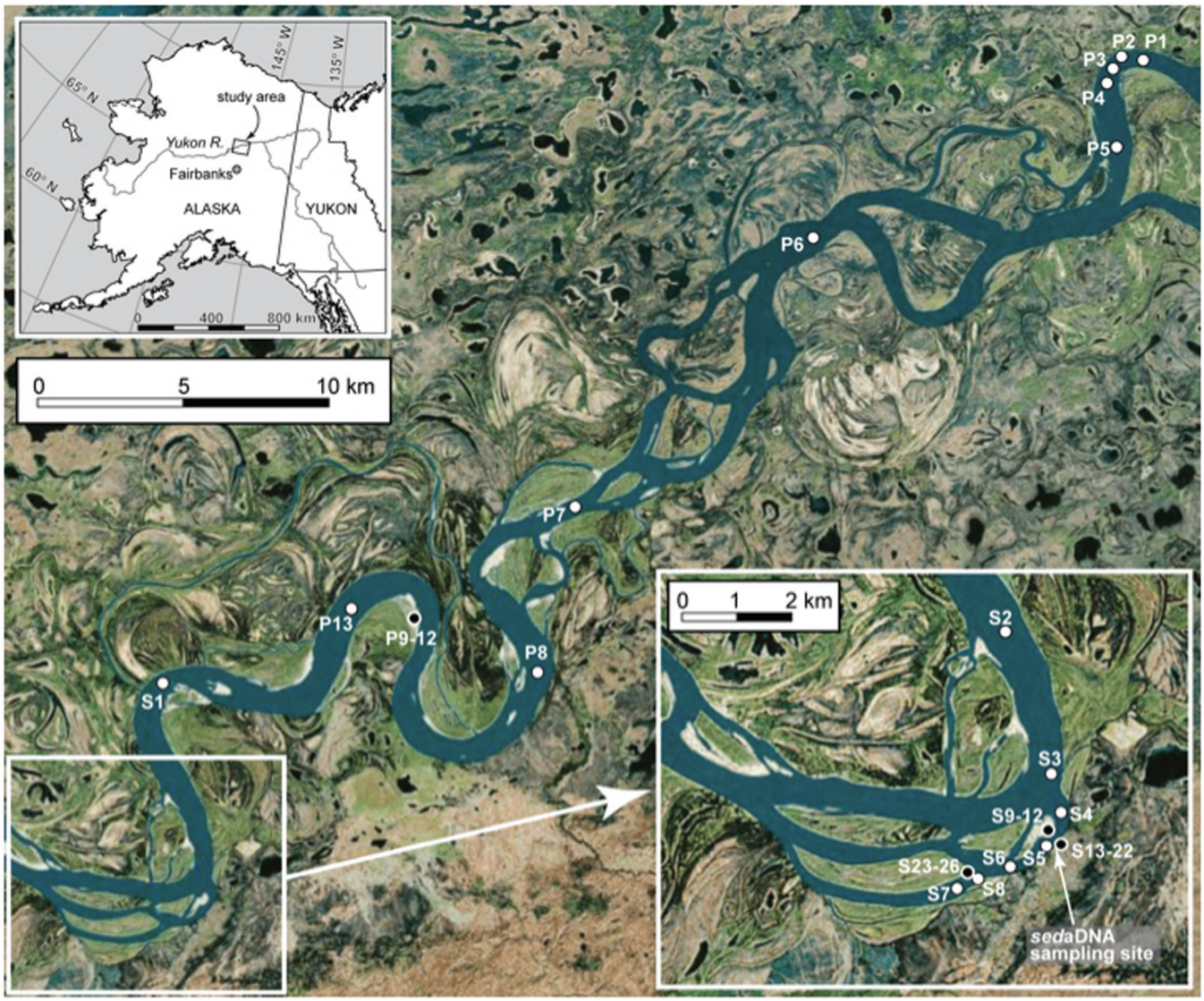

Fig. S4. Location of modern river water and surface sediment samples in the Yukon Flats. Upper inset map shows location of lower Yukon Flats in Alaska. Lower inset photo shows sample locations nearest the *sed*aDNA sampling site at the Stevens Village exposure. Surface sediment and Yukon River water samples are indicated by black and white dots, respectively. Sample descriptions and geographic coordinates are given in Table S5. Yukon River flows from upper-right to lower-left. Satellite imagery courtesy of Geographic Information Network of Alaska (www.gina.alaska.edu).

Table S1. Conventional and calibrated (calendar-year) radiocarbon ages of plant macrofossils from Stevens Village exposure

Laboratory number	Age, ^{14}C yr BP	Calibrated age,* yr BP	Material	Sample elevation, m a.r.l.
GSC-6735	6,950 ± 80	7,625–7,945	*Picea* wood	13.7
GSC-6690	6,990 ± 80	7,675–7,960	*Picea* wood	13.7
GSC-6734	6,800 ± 70	7,515–7,790	*Picea* wood	13.0
GSC-6731	6,950 ± 70	7,670–7,935	*Picea* wood	13.0
GSC-6665	7,110 ± 100	7,725–8,160	*Picea* wood	13.0
UCIAMS-26579	9,210 ± 25	10,260–10,490	*Rubus* sp. nutlets	11.0
AA-52065	8,320 ± 200	8,650–9,700	Wood	9.5
UCIAMS-36647	9,505 ± 30	10,670–11,070	Wood	9.0
GSC-6718	9,450 ± 120	10,300–11,170	Shrub wood (in situ)	5.2
GSC-6707	9,660 ± 110	10,700–11,250	Shrub wood (in situ)	5.2
AA-52066	9,752 ± 85	10,780–11,330	Shrub wood (in situ)	5.2
AA-52061	9,813 ± 91	10,805–11,610	Wood	4.0
AA-52060	9,830 ± 130	10,780–11,760	Wood	4.0

m a.r.l., meters above river level.
*2σ (95%) range, calibrated using Calib 5.0.2.

Table S2. Dose rate data, equivalent dose (D_e) estimates, and OSL ages for Stevens Village samples

Sample code	Sample depth, m	Water/ organic content, %	Radionuclide concentrations			Total dose rate, Gy/ka	No. of grains	Overdispersion, %	Age model	D_e, Gy	OSL age, ka
			^{238}U, μg/g	^{232}Th, μg/g	^{40}K, %						
SV30	2.5	26/6	3.6 ± 0.1	9.0 ± 0.3	1.25 ± 0.04	2.16 ± 0.12	40/1200	69 ± 9	MAM-4	22.7 ± 4.4	10.5 ± 2.1
SV28	4.4	19/5	3.6 ± 0.1	9.9 ± 0.3	1.26 ± 0.04	2.34 ± 0.12	48/1300	75 ± 9	MAM-4	29.3 ± 4.3	12.5 ± 1.9
SV26	6.2	14/5	3.7 ± 0.1	8.1 ± 0.2	1.25 ± 0.04	2.35 ± 0.17	68/1700	80 ± 8	MAM-4	31.4 ± 4.6	13.4 ± 2.2

Sample depth, depth below modern ground surface. Water/organic content, field water content/mass of organic matter (determined by loss on ignition), expressed as percent dry mass of mineral fraction and assigned relative uncertainties of ±10%. Measurements of Radionuclide concentrations were made on dried and powdered samples by INAA and ICP-OES. U, Th and K concentrations were assigned relative uncertainties of ± 3% for beta dose rates (based on the typical variability between replicate measurements) and 10% for gamma dose rates (to accommodate any spatial heterogeneity in the gamma radiation field). Values for Total dose rate, D_e, and OSL age are expressed as mean ± total uncertainty (68% confidence interval), calculated as the quadratic sum of the random and systematic uncertainties. Total dose rate includes cosmic-ray dose rates of 0.11–0.16 Gy/ka (at field water content) and internal dose rate of 0.03 Gy/ka, with relative uncertainties of ± 10% and ± 30%, respectively. Values for No. of grains indicate the number of single grains used for D_e determination/total number of grains analyzed. Overdispersion percentages represent the relative standard deviations of the equivalent-dose distributions after allowing for measurement uncertainties. Age model, 4-parameter version of the minimum age model (MAM-4) used to calculate the sample equivalent dose. Before running the model, a relative error of 15% was added in quadrature to each D_e. OSL age, expressed in thousands of calendar years ago. The total uncertainty of OSL age estimates includes a systematic component of ±2% associated with laboratory beta-source calibration.

Table S3. PCR primers and sequences, with references, annealing temperatures, and approximate product length (base pairs, bp)

Name	Sequence	Source	Annealing temperature, °C	Product length, bp
16Smam1	5′- CGGTTGGGGTGACCTCGGA	Ref. 33	60	91
16Smam2	5′- GCTGTTATCCCTAGGGTAACT	Ref. 33		
16Smam3	5′- TGGGGTGACCTCGGAGAAY	This study	57	78
16Smam4	5′- TCAACGGAMCAAGTTACCCTA	This study		
Mammoth CRF1	5′- CATGCTTATAAGCAAGTACTGT	This study	56	165
Mammoth CRR1	5′- TGAGAAATCTCTAGTCATCATG	This study		

Table S4. Mammoth macrofossil remains used in the statistical analyses

Laboratory ID number	Genus	Species	^{14}C age	1σ error	Region	Locality	Ref.
AA-22573	*Mammuthus*	*primigenius*	11,500	160	Alaska	Galena	(34)
AA-17601	*Mammuthus*	—	11,540	140	Alaska	Delta, Charles Holmes (Swan Pt. Site)	(35)
AA-17559	*Mammuthus*	*primigenius*	11,860	120	Yukon Territory	Dawson area	(34)
AA-26006	*Mammuthus*	*primigenius*	11,910	130	Alaska	Cape Lisborn	(34)
AA-17526	*Mammuthus*	—	11,990	130	Yukon Territory		(35)
AA-14940	*Mammuthus*	*primigenius*	12,123	88	Alaska	Goldstream	(34)
AA-17614	*Mammuthus*	*primigenius*	12,190	130	Alaska	Ikpikpuk	(34)
CRNL-1220-b	*Mammuthus*	sp.	12,190	500	Yukon Territory	Bluefish Cave I	(36)
AA-14938	*Mammuthus*	*primigenius*	12,337	108	Alaska	Cleary Cr.	(34)
AA-14860	*Mammuthus*	*primigenius*	12,429	178	Alaska	Engineer Cr.	(34)
AA-26017	*Mammuthus*	*primigenius*	12,440	130	Alaska	Cap.Princ. Wh.	(34)
AA-14916	*Mammuthus*	*primigenius*	12,476	81	Alaska	Cleary Cr.	(34)
AA-14954	*Mammuthus*	*primigenius*	12,490	170	Alaska	Ikpikpuk	(34)
AA-14357	*Mammuthus*	*primigenius*	12,508	145	Alaska	Escholtz Bay	(34)
AA-14880	*Mammuthus*	*primigenius*	12,576	147	Alaska	Goldstream	(34)
CAMS-17045	*Mammuthus*	sp.	12,606	70	Alaska	Swan Point site	(36)
AA-14888	*Mammuthus*	*primigenius*	12,677	142	Alaska	Sullivan Cr.	(34)
Beta-9906	*Mammuthus*	sp.	12,980	250	Alaska	Colorado Creek	(36)
AA-14947	*Mammuthus*	*primigenius*	13,060	150	Alaska	Goldstream	(34)
CRNL-1220-a	*Mammuthus*	sp.	13,070	400	Yukon Territory	Bluefish Cave I	(36)
AA-14925	*Mammuthus*	*primigenius*	12,926	85	Alaska	40 mi	(34)
AA-14949	*Mammuthus*	*primigenius*	13,250	170	Alaska	St. Lawrence	(34)
CRNL-1220-c	*Mammuthus*	sp.	13,280	390	Yukon Territory	Bluefish Cave I	(36)
AA-26028	*Mammuthus*	*primigenius*	13,290	140	Alaska	Point Hope	(34)
AA-14346	*Mammuthus*	*primigenius*	13,315	201	Alaska	St. Lawrence	(34)
CRNL-1218	*Mammuthus?*	sp.	13,335	390	Yukon Territory	Old Crow River	(36)
AA-14867	*Mammuthus*	*primigenius*	13,339	150	Alaska	Goldstream	(34)
DIC-2130	*Mammuthus*	*primigenius*	13,340	115	Alaska	Teklanika River	(37)
AA-14944	*Mammuthus*	*primigenius*	13,380	88	Alaska	Chena	(34)
AA-14883	*Mammuthus*	*primigenius*	13,410	152	Alaska	Ester Cr.	(34)
AA-14934	*Mammuthus*	*primigenius*	13,436	87	Alaska	Cleary Cr.	(34)
QL-1365	*Mammuthus*	sp.	13,500	100	Alaska	Teklanika Valley	(36)
AA-14889	*Mammuthus*	*primigenius*	13,661	156	Alaska	Dome Cr.	(34)
AA-25999	*Mammuthus*	*primigenius*	13,690	190	Alaska	Ruby	(34)
Beta-29166	*Mammuthus*	sp.	13,725	110	Alaska	Lower Rampart cave	(36)
Beta-13867	*Mammuthus*	*primigenius*	13,820	340	Yukon Territory	Old Crow River	(36)
RIDDL-559	*Mammuthus*	*primigenius*	13,940	160	Yukon Territory	Bluefish Cave I	(36)
AA-14895	*Mammuthus*	*primigenius*	14,023	98	Alaska	Fairbanks Cr.	(34)
AA-14892	*Mammuthus*	*primigenius*	14,093	163	Alaska	Cleary Cr.	(34)
AA-14900	*Mammuthus*	*primigenius*	14,115	88	Alaska	Ester Cr.	(34)
AA-26033	*Mammuthus*	*primigenius*	14,260	160	Alaska	Escholtz Bay	(34)
Beta-20027	*Mammuthus*	sp.	14,270	950	Alaska	Trail Creek Cave	(36)
AA-26002	*Mammuthus*	*primigenius*	14,300	170	Alaska	Ruby	(34)
AA-14919	*Mammuthus*	*primigenius*	14,372	92	Alaska	Dome Cr.	(34)
AA-14923	*Mammuthus*	*primigenius*	14,390	92	Alaska	Cleary Cr.	(34)
AA-14882	*Mammuthus*	*primigenius*	14,679	174	Alaska	Ban Cr.	(34)
AA-26030	*Mammuthus*	*primigenius*	14,760	170	Alaska	Ruby	(34)
AA-26000	*Mammuthus*	*primigenius*	14,830	180	Alaska	St. Michaels	(34)
B-5691	*Mammuthus*	*primigenius*	15,090	170	Alaska	Colorado Creek	(37)
AA-14912	*Mammuthus*	*primigenius*	15,102	135	Alaska	Cleary Cr.	(34)
Beta-16996	*Mammuthus*	sp.	15,280	120	Alaska	Colorado Creek	(36)
AA-14932	*Mammuthus*	*primigenius*	15,373	101	Alaska	Ban Cr.	(34)
SI-453	*Mammuthus*	*primigenius*	15,380	300	Alaska	Fairbanks Creek	(36)
AA-14941	*Mammuthus*	*primigenius*	15,426	98	Alaska	Goldstream	(34)
AA-14920	*Mammuthus*	*primigenius*	15,453	99	Alaska	Ban Cr.	(34)
GSC-3053	*Mammuthus* cf.	*primigenius*	15,500	130	Yukon Territory	Bluefish Cave II	(36)
AA-14910	*Mammuthus*	*primigenius*	15,513	192	Alaska	Cleary Cr.	(34)
AA-14894	*Mammuthus*	*primigenius*	15,540	145	Alaska	Ban Cr	(34)
AA-22619	*Mammuthus*	*primigenius*	15,654	218	Alaska		(34)
AA-26015	*Mammuthus*	*primigenius*	15,740	230	Alaska	Point Hope	(34)
AA-14872	*Mammuthus*	*primigenius*	15,796	195	Alaska	Goldstream	(34)
Beta-67690	*Mammuthus*	sp.	15,830	70	Alaska	Shaw creek	(36)
AA-14915	*Mammuthus*	*primigenius*	15,917	106	Alaska	Fairbanks Cr.	(34)

Laboratory ID number	Genus	Species	^{14}C age	1σ error	Region	Locality	Ref.
AA-14928	*Mammuthus*	*primigenius*	15,947	121	Alaska	Goldstream	(34)
GSC-1893	*Mammuthus*	sp.	16,100	130	Yukon Territory	Scroggie Creek	(36)
AA-683	*Mammuthus*	sp.	16,150	230	Alaska	Colorado Creek	(36)
AA-14866	*Mammuthus*	*primigenius*	16,168	209	Alaska	Cleary Cr.	(34)
AA-17576	*Mammuthus*	*primigenius*	16,170	210	Alaska	Alaska	(34)
AA-14899	*Mammuthus*	*primigenius*	16,243	105	Alaska	Fox	(34)
AA-14364	*Mammuthus*	*primigenius*	16,319	292	Alaska	Inglutalik Cr.	(34)
AA-14955	*Mammuthus*	*primigenius*	16,370	210	Alaska	St. Lawrence Is.	(34)
AA-14896	*Mammuthus*	*primigenius*	16,789	108	Alaska	Ester Cr.	(34)
SI-2823 AP	*Mammuthus*	sp.	16,880	250	Yukon Territory	Old Crow River	(36)
AA-17571	*Mammuthus*	*primigenius*	16,940	210	Alaska	Amer. R. AK	(34)
AA-14936	*Mammuthus*	*primigenius*	17,354	143	Alaska	Goldstream	(34)
AA-14922	*Mammuthus*	*primigenius*	17,437	132	Alaska	Goldstream	(34)
CRNL-1221 + 1221a + 1221b	*Mammuthus*	*primigenius*	17,880	270	Yukon Territory	Bluefish Cave II	(36)
Beta-70099	*Mammuthus*	*primigenius*	17,950	120	Yukon Territory	Gold Run Creek	(36)
AA-14890	*Mammuthus*	*primigenius*	18,041	275	Alaska	Ester Cr.	(34)
AA-26004	*Mammuthus*	*primigenius*	18,090	250	Alaska	Southeast AK	(34)
AA-14956	*Mammuthus*	*primigenius*	18,120	260	Alaska	St. Lawrence Is	(34)
AA-26021	*Mammuthus*	*primigenius*	18,140	280	Alaska	Yuk Palisades	(34)
AA-14935	*Mammuthus*	*primigenius*	18,379	124	Alaska	Cleary Cr.	(34)
USGS-1485	*Mammuthus*	sp.	18,560	70	Alaska	Epiguruk	(36)
AA-14350	*Mammuthus*	*primigenius*	18,691	427	Alaska	St. Lawrence	(34)
AA-14918	*Mammuthus*	*primigenius*	19,011	132	Alaska	Sulllivan Cr.	(34)
USGS-1439	*Mammuthus*	sp.	19,060	90	Alaska	Epiguruk	(36)
SI-2812 AP	*Mammuthus*	sp.	19,080	280	Yukon Territory	Old Crow River	(36)
AA-14897	*Mammuthus*	*primigenius*	19,169	138	Alaska	Long Cr.	(34)
I-8578	*Mammuthus* cf.	*primigenius*	19,440	290	Northwest Territories	Tununuk	(36)
AA-14344	*Mammuthus*	*primigenius*	19,447	162	Alaska	St. Lawrence	(34)
AA-14929	*Mammuthus*	*primigenius*	19,477	173	Alaska	Fairbanks Cr.	(34)
SI-2814 AP	*Mammuthus*	sp.	19,520	470	Yukon Territory	Old Crow River	(36)
AA-17620	*Mammuthus*	*primigenius*	19,560	330	Alaska	Ikpikpuk	(34)
AA-14348	*Mammuthus*	*primigenius*	19,759	197	Alaska	St. Lawrence	(34)
AA-14356	*Mammuthus*	*primigenius*	19,763	307	Alaska	Koyuk	(34)
AA-26018	*Mammuthus*	*primigenius*	19,870	310	Alaska	Kotzebu. Snd.	(34)
AA-14924	*Mammuthus*	*primigenius*	19,878	141	Alaska	Long Cr.	(34)
AA-17623	*Mammuthus*	*primigenius*	19,970	350	Alaska	Ikpikpuk	(34)
AA-26003	*Mammuthus*	*primigenius*	20,120	350	Alaska	Port Clarence	(34)
I-10971	*Mammuthus*	*columbi*	20,190	400	Yukon Territory	Quartz Creek	(36)
RIDDL-223	*Mammuthus*	*primigenius*	20,230	180	Yukon Territory	Bluefish Cave II	(36)
RIDDL-330	*Mammuthus*	*primigenius*	20,230	181	Yukon Territory	Bluefish Cave II	(36)
TO-2355	cf. *Mammuthus*	sp.	20,270	270	Northwest Territories	Banks Island	(36)
AA-14960	*Mammuthus*	*primigenius*	20,350	330	Alaska	Long Cr.	(34)
AA-26035	*Mammuthus*	*primigenius*	20,780	340	Alaska	Kotzebue Snd.	(34)
DIC-1333	*Mammuthus*	*primigenius*	21,050	310	Alaska	Porcupine Cave	(37)
L-601	*Mammuthus*	*primigenius*	21,300	1300	Alaska	Fairbanks area	(36)
AA-14349	*Mammuthus*	*primigenius*	21,331	633	Alaska	St. Lawrence	(34)
GSC-1760–2	cf. *Mammuthus*	sp.	21,600	230	Nunavut	Melville Island	(36)
AA-14943	*Mammuthus*	*primigenius*	21,705	180	Alaska	Goldstream	(34)
AA-14917	*Mammuthus*	*primigenius*	21,848	175	Alaska	Cleary Cr.	(34)
GSC-1760	*Mammuthus*	*primigenius*	21,900	320	Alaska	Melville	(37)
AA-14345	*Mammuthus*	*primigenius*	22,399	253	Alaska	St. Lawrence	(34)
RIDDL-558	*Mammuthus*	*primigenius*	22,430	260	Yukon Territory	Bluefish Cave II	(36)
I-3573	*Mammuthus*	sp.	22,600	600	Yukon Territory	Old Crow River	(36)
CAMS-23470	*Mammuthus*	*primigenius*	22,740	90	Yukon Territory	Bluefish Cave II	(36)
AA-14951	*Mammuthus*	*primigenius*	22,760	430	Alaska	Alaskan	(34)
AA-14873	*Mammuthus*	*primigenius*	22,796	456	Alaska	Goldstream	(34)
V-48–152	*Mammuthus*	*primigenius*	22,850	250	Alaska	Colorado Creek	(37)
AA-14868	*Mammuthus*	*primigenius*	23,015	449	Alaska	Goldstream	(34)
AA-17574	*Mammuthus*	*primigenius*	23,150	460	Alaska	Tanana AK	(34)
RIDDL-225	*Mammuthus*	*primigenius*	23,200	250	Yukon Territory	Bluefish Cave II	(36)
AA-14864	*Mammuthus*	*primigenius*	23,222	453	Alaska	Goldstream	(34)
USGS-1438	*Mammuthus*	*primigenius*	23,620	110	Alaska	Epiguruk	(36)
AA-14881	*Mammuthus*	*primigenius*	23,808	487	Alaska	Gilmore Cr.	(34)
RIDDL-224	*Mammuthus*	*primigenius*	23,910	200	Yukon Territory	Bluefish Cave II	(36)

Laboratory ID number	Genus	Species	^{14}C age	1σ error	Region	Locality	Ref.
AA-26013	*Mammuthus*	*primigenius*	24,193	510	Alaska	Point Hope	(34)
AA-14854	*Mammuthus*	*primigenius*	24,249	521	Alaska	Inglutalik	(34)
AA-14347	*Mammuthus*	*primigenius*	24,609	247	Alaska	St. Lawrence	(34)
RIDDL-229	*Mammuthus* ?	sp.	24,700	250	Yukon Territory	Cadzow Bluff	(36)
AA-14933	*Mammuthus*	*primigenius*	24,730	224	Alaska	Goldstream	(34)
CRNL-1232	*Mammuthus* ?	sp.	25,170	630	Yukon Territory	Cadzow Bluff	(36)
RIDDL-191	*Mammuthus*	sp.	25,200	400	Yukon Territory	Old Crow River	(36)
RIDDL-306	*Mammuthus*	sp.	25,250	300	Yukon Territory	Old Crow River	(36)
AA-14870	*Mammuthus*	*primigenius*	25,362	584	Alaska	Cleary Cr.	(34)
RIDDL-193	*Mammuthus*	sp.	25,450	450	Yukon Territory	Old Crow River	(36)
AA-22577	*Mammuthus*	*primigenius*	25,560	600	Alaska	Rampart	(34)
RIDDL-300	*Mammuthus* ?	sp.	25,600	300	Yukon Territory	Old Crow River	(36)
RIDDL-303	*Mammuthus* ?	sp.	25,620	300	Yukon Territory	Old Crow River	(36)
I-8583	*Mammuthus* cf.	*primigenius*	25,680	580	Yukon Territory	Hunker Creek	(36)
SI-2818 CO	*Mammuthus*	sp.	25,910	680	Yukon Territory	Old Crow River	(36)
CRNL-1234	*Mammuthus?*	sp.	25,970	560	Yukon Territory	Old Crow River	(36)
AA-14855	*Mammuthus*	*primigenius*	26,022	640	Alaska	Cripple Cr.	(34)
AA-26022	*Mammuthus*	*primigenius*	26,050	690	Alaska	Nulato	(34)
AA-17569	*Mammuthus*	*primigenius*	26,800	690	Yukon Territory	Dawson area	(34)
RIDDL-232	*Mammuthus* ?	sp.	27,000	400	Yukon Territory	Old Crow River	(36)
RIDDL-192	*Mammuthus*	sp.	27,100	800	Yukon Territory	Old Crow River	(36)
AA-26029	*Mammuthus*	*primigenius*	27,180	730	Alaska	Point Clarence	(34)
AA-26012	*Mammuthus*	*primigenius*	27,360	770	Alaska	Elephant Pt.	(34)
AA-14930	*Mammuthus*	*primigenius*	27,436	308	Alaska	Fairbanks area	(34)
AA-17549	*Mammuthus*	*primigenius*	27,490	750	Yukon Territory	Dawson area	(34)
GX-1568-Du	*Mammuthus*	sp.	27,500	1800	Yukon Territory	Old Crow River	(36)
SI-2812 CO	*Mammuthus*	sp.	27,700	460	Yukon Territory	Old Crow River	(36)
AA-17566	*Mammuthus*	*primigenius*	28,400	840	Yukon Territory	Dawson area	(34)
AA-25997	*Mammuthus*	*primigenius*	28,440	850	Alaska	Bristol Bay	(34)
RIDDL-305	*Mammuthus*	sp.	28,600	350	Yukon Territory	Old Crow River	(36)
RIDDL-301	*Mammuthus*	sp.	28,780	350	Yukon Territory	Old Crow River	(36)
RIDDL-130	cf. *Mammuthus*	sp.	28,800	450	Yukon Territory	Old Crow River	(36)
GX-5740-a	*Mammuthus*	sp.	28,920	2250	Alaska	Bering Sea coast area	(36)
GX-1567	*Mammuthus* cf.	*primigenius*	29,100	3000	Yukon Territory	Old Crow	(36)
I-11050	cf. *Mammuthus*	sp.	29,300	1200	Yukon Territory	Old Crow River	(36)
DIC-1819	*Mammuthus*	sp.	29,450	610	Alaska	Tyone River	(36)
AA-17538	*Mammuthus*	*primigenius*	30,000	1000	Yukon Territory	Eldorado Cr.	(34)

Level of taxa identification, specimen age, fossil locality and region, and literature reference are provided.

Table S5. Sample identification numbers, field codes, descriptions and locations of control samples of Yukon River water and surface sediments

Sample	Field Code	Description	Latitude, °N	Longitude, °W
S1	09-SV-1	River water US of SV	66.053	148.989
S2	09-SV-2	River water US of SV	66.018	148.968
S3	09-SV-3	River water US of SV	65.995	148.952
S4	09-SV-4	River water at US edge of SV	65.988	148.949
S5	09-SV-5	River water below SV measured section	65.983	148.956
S6	09-SV-6	River water at DS edge of SV	65.980	148.972
S7	09-SV-7	River water DS of SV	65.976	148.996
S8	09-SV-8	River water DS of SV	65.978	148.985
S9	09-SV-9	Sediments on river bar across from SV measured section	65.985	148.955
S10	09-SV-10	Sediments on river bar across from SV measured section	65.985	148.955
S11	09-SV-11	Sediments on river bar across from SV measured section	65.985	148.955
S12	09-SV-12	Sediments on river bar across from SV measured section	65.985	148.955
S13	09-SV-13	O horizon at site 1, near top of SV measured section	65.983	148.955
S14	09-SV-14	A horizon at site 1, near top of SV measured section	65.983	148.955
S15	09-SV-15	O horizon at site 2, near top of SV measured section	65.983	148.955
S16	09-SV-16	A horizon at site 2, near top of SV measured section	65.983	148.955
S17	09-SV-17	O horizon at site 3, near top of SV measured section	65.983	148.955
S18	09-SV-18	A horizon at site 3, near top of SV measured section	65.983	148.955
S19	09-SV-19	O horizon at site 4, near top of SV measured section	65.983	148.955
S20	09-SV-20	A horizon at site 4, near top of SV measured section	65.983	148.955
S21	09-SV-21	O horizon at site 5, near top of SV measured section	65.983	148.955
S22	09-SV-22	A horizon at site 5, near top of SV measured section	65.983	148.955
S23	09-SV-23	Sediments on river bar DS from SV measured section	65.978	148.985
S24	09-SV-24	Sediments on river bar DS from SV measured section	65.978	148.985
S25	09-SV-25	Sediments on river bar DS from SV measured section	65.978	148.985
S26	09-SV-26	Sediments on river bar DS from SV measured section	65.978	148.985
P1	09-PU-1	River water US of PU	66.249	148.240
P2	09-PU-2	River water at US edge of PU	66.248	148.255
P3	09-PU-3	River water below PU measured section	66.247	148.260
P4	09-PU-4	River water at DS edge of PU	66.246	148.264
P5	09-PU-5	River water DS of PU	66.217	148.257
P6	09-PU-6	River water between PU and SV	66.187	148.504
P7	09-PU-7	River water between PU and SV	66.109	148.662
P8	09-PU-8	River water between PU and SV	66.056	148.706
P9	09-PU-9	Sediments on river bar between PU and SV	66.066	148.796
P10	09-PU-10	Sediments on river bar between PU and SV	66.066	148.796
P11	09-PU-11	Sediments on river bar between PU and SV	66.066	148.796
P12	09-PU-12	Sediments on river bar between PU and SV	66.066	148.796
P13	09-PU-13	River water between PU and SV	66.077	148.847

US, upstream; DS, downstream; PU, Purgatory bluff; SV, Stevens Village bluff *sed*aDNA sampling site.